Nucleic Acids Research, Vol. 18, No. 1

New photoactivatable structural and affinity probes of RNAs: specific features and applications for mapping of spermine binding sites in yeast $tRNA^{Asp}$ and interaction of this tRNA with yeast aspartyl-tRNA synthetase

Angela Garcia, Richard Giegé and Jean-Paul Behr*
Laboratoire de Biochimie, Institut de Biologie Moléculaire et Cellulaire du CNRS, 15 rue René Descartes, 67084 Strasbourg Cedex, France

Received October 3, 1989; Revised and Accepted November 30, 1989

ABSTRACT

Aryldiazonium salts are shown to be useful as phototriggered structural probes for RNA mapping as well as for footprinting of RNA/protein interaction. In particular the yeast $tRNA^{Asp}$/aspartyl-tRNA synthetase complex is shown to involve the variable loop face and the concave side of the L-shaped nucleic acid bound to a lipophilic area of the enzyme. When chemically linked to spermine, the photoactive group cleaves RNA at polyamine binding sites ; 3 – 4 spermines have been located in the $tRNA^{Asp}$, stabilizing the central part of the molecule in regions where two ribose-phosphate strands are close to each other.

INTRODUCTION

Mapping of nucleic acids with chemical probes has become in recent years a powerful methodology to gain insight into solution conformational features of these macromolecules, either free (e.g. 1–3) or complexed with proteins (e.g. 4–7). One reason for the extensive development of solution mapping relies in the possibility to analyze the chemical modification data by rapid sequencing methodologies of nucleic acids (8, 9), implying that modifications occur at most once per nucleic acid molecule and lead to chain break at the modified positions only. However, many such probes have to be used under conditions which can be harmful for the nucleic acid (or for the protein in nucleic acid complexes), such as high concentrations, long reaction times or rather alkaline pH. Therefore, there is a search for new reactive chemical functionalities which would overcome these problems. From another point of view, the design of probes with new specificities would enlarge the field of structural and conformational mapping of nucleic acids.

Here we describe a family of photoactivatable structural probes with novel specificities for nucleic acids. They possess an aryldiazonium group as the reactive center and fulfill the requirements discussed above. The probes were designed by linking these groups to polyamines, thus leading to preferential cleavage of the nucleic acids at the binding sites (10). Cleavage can be obtained with very low concentrations of reagent after affinity binding. A simplified version, consisting of the aryldiazonium center alone, was synthesized as a photochemically triggered ethylnitrosourea substitute, for classical experiments conducted in a statistical and non specific fashion (ethylnitrosourea is a phosphate alkylating probe leading to breakage of the ribose-phosphate chain in RNAs (e.g. 6)). The target molecule was yeast $tRNA^{Asp}$, for which a high resolution crystal structure is known (11,12), but where precise structural data about aspartyl-tRNA synthetase or polyamine binding are lacking.

MATERIALS AND METHODS

Synthesis of structural probes

The p-diazonium anilides of L-2-carboxyputrescine (PuN_2^{3+}) and L-5-carboxyspermine ($SperN_2^{5+}$) were prepared as described in (10) ; the p-N-dimethylaminobenzenediazonium salt, abbreviated $BenzN_2^+$, was prepared as described in (13). Probes were stored in the dark as ammonium salts. The extinction coefficients for the diazonium anilides and $BenzN_2^+$ are $\epsilon = 2.25\ 10^4\ dm^3 \cdot mol^{-1} \cdot cm^{-1}$ at 323 nm and $3.75\ 10^4\ dm^3 \cdot mol^{-1} \cdot cm^{-1}$ at 379 nm, respectively. The chemical structures of the various probes used in this work are depicted in Fig. 1.

Transfer RNA, enzymes and chemicals

Yeast $tRNA^{Asp}$ was isolated from total brewer's yeast tRNA (Boehringer, Mannheim, FRG) by counter-current distribution (14), followed by chromatographies on benzoylated DEAE-cellulose and on Sepharose-4B (15, 16). Yeast aspartyl-tRNA synthetase was prepared according to (17) and as modified in (18). Concentrations were determined spectrophotometrically (one optical density unit at 260 nm corresponds to 40 μg tRNA/ml in a 1 cm path-lengh cell, and to 0.6 mg aspartyl-tRNA synthetase/ml at 280 nm). Calf intestinal phosphatase and snake venom phosphodiesterase were from Worthington (Freehold, USA) ; phage T_4 polynucleotide kinase was from Amersham

* To whom correspondence should be addressed at Laboratoire de Chimie Organique Physique, URA 422 du CNRS, Institut Le Bel, Université Louis Pasteur, 4 rue Blaise Pascal, 67000 Strasbourg, France

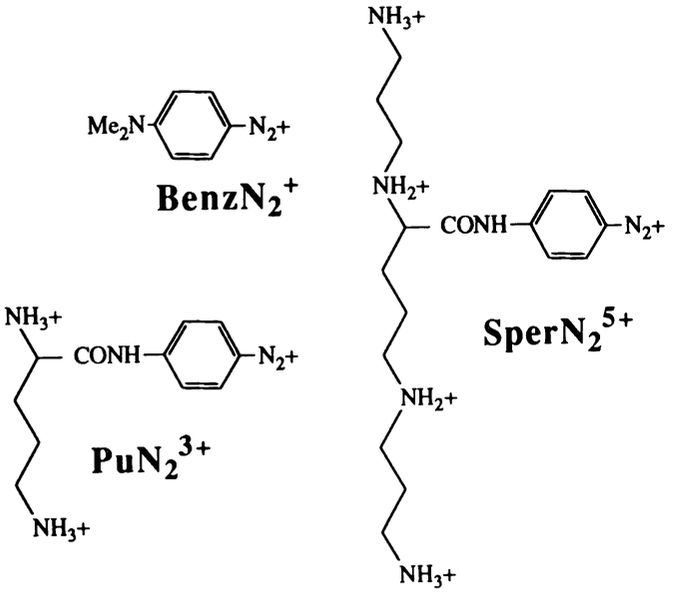

Fig. 1. Structure of the photochemical probes : p-N-dimethylamino-benzenediazonium ($BenzN_2^+$), p-diazonium anilide of L-2-carboxyputrescine (PuN_2^{3+}), p-diazonium anilide of L-5-carboxyspermine ($SperN_2^{5+}$).

France (Versailles) ; tRNA nucleotidyl-transferase was prepared from commercial baker's yeast (FALA, Strasbourg, France) according to (19) ; ribonuclease T_1 and U_2, were from Pharmacia France (Les Ulis). Radioactive nucleotides, [α-^{32}P] ATP at 410 Ci/mmol and [γ-^{32}P] ATP at 3200 Ci/mmol, were from Amersham. L-[U-^{14}C] Aspartic acid at 8.14 Ci/mol was from the Commissariat à l'Energie Atomique (Saclay, France).

End-labelling of tRNA

Transfer RNA was labelled either at its 5′ or 3′ end ; labelling at the 5′ end with [γ-^{32}P] ATP was performed by phage T_4 polynucleotide kinase on samples previously dephosphorylated with alkaline phosphatase (20). For 3′ end-labelling, tRNA was first deprived of its CCA-end sequence by snake venom phosphodiesterase, this sequence being reconstituted in the presence of cold CTP, [α-^{32}P] ATP and tRNA nucleotidyl-transferase (2). Labelled tRNAs were purified by high voltage gel electrophoresis in 15% (w/v) polyacrylamide/8M urea gels.

Photochemical cleavage

Cold $tRNA^{Asp}$ was added to labelled $tRNA^{Asp}$ to achieve a total concentration of 4 μM and 10^5 cpm in 10 μl. For footprinting experiments on complexes, yeast aspartyl-tRNA synthetase was added at a concentration of 8 μM (without additional magesium), which ensures nearly complete binding (> 95 %) of the substrate ($K_A = 6.10^8$ M^{-1}, without magnesium) (21). A 10 min pre-incubation was made prior to addition of the photochemical reagent.

Reactions with tRNA alone were performed at room temperature in 50 mM sodium acetate buffer pH 6.0 (buffers consisting of strong nucleophiles reacted slowly with the probes (22) and Mg^{2+} showed some inhibitory effect above millimolar concentration). For experiments with aspartyl-tRNA synthetase, samples of 5 μl free tRNA in 100 mM sodium acetate at pH 6.0 were supplemented with 2.5 μl of aspartyl-tRNA synthetase in its conservating buffer (50 mM Tris-HCl pH 7.5, 0.1 mM EDTA, 0.1 mM dithioerythritol, 50% glycerol) and 2.5 μl of an aqueous solution containing the probe. The reference samples were run by adding 2.5 μl of conservating buffer without the synthetase. It was verified that the final pH was 6.0. Reagents were added at final concentrations ranging from 4 to 40 μM for polyamines probes and 0.04 to 10 mM for the $BenzN_2^+$ probe. Incubation mixtures were immediately illuminated with an U.V. and I.R. filtered 500 W xenon lamp for 10 sec. Samples without protein were dried under vacuum and the dry pellets dissolved in 4 μl of 10 mM $MgCl_2$, in order to prevent aggregation or coprecipitation of tRNA fragments with polyamines which would result in a loss of RNA material during the electrophoretic step. For control experiments, probe solutions were replaced by an equal volume of buffer.

Samples for footprinting experiments were submitted to phenol extraction followed by ether treatment. Transfer RNA (*ca.* 100 μl) was precipitated with three volumes of ethanol, and the pellets washed twice with cold ethanol. Subsequent workup was similar to that of samples containing tRNA alone. Inactivation of aspartyl-tRNA synthetase in the footprinting conditions was evaluated in the presence of the highest photochemical reagent concentrations used, by aminoacylation in a buffer containing 50 mM Tris-HCl pH 7.5, 10 mM ATP, 15 mM $MgCl_2$, 2.5 mM glutathione, 30 mM KCl, 80 μM crude brewer's yeast tRNA, 0.1mg/ml bovine serum albumin and 0.1 mM L-[U-^{14}C] aspartic acid.

Analysis of cleavage positions

For each run, equal amounts of radioactivity (counted by Cerenkov effect) for each sample were loaded on a 15% polyacrylamide sequencing gel. After electrophoresis, the sites of splitting were assigned by comparison with ribonuclease T_1 and U_2, as well as with formamide hydrolysis ladders. Because of the resolution of the gels, the 3′ and 5′ termini of the tRNA could not be mapped with accuracy.

RESULTS AND DISCUSSION

New photochemical probes and methodological aspects

(i) Specific features of the probes : The polycationic *affinity* probes ($SperN_2^{5+}$, PuN_2^{3+}) are composed of an arenediazonium group linked to spermine or putrescine. Their design relied on the following properties : (i) photochemical cleavage of the ribose-phosphate backbone under rapid and simple handling conditions and (ii) strong and specific interaction with nucleic acids (23) so that an affinity-type binding of the reagent would allow reaction with the RNA at very low concentrations of the probe. However, analysis of the modification by rapid RNA sequencing methods requires that cleavage occurs less than once per RNA molecule. Therefore, only the strongest polyamine sites can be mapped accurately at concentrations in the range of their K_D; at higher probe concentrations, where lower affinity sites may be occupied, the probability of multiple cleavages increases.

The photochemical *structural* probe $BenzN_2^+$, which has been used as a protein labelling agent (13, 24), should not have a special affinity for nucleic acids. Thus, it is anticipated that RNA cleavage promoted by $BenzN_2^+$ will occur at much higher concentrations than that induced by the modified polyamines. As will be shown below, the properties of $BenzN_2^+$ make it a valuable substitute of phosphate alkylating reagents such as ethylnitrosourea, for structure mapping of RNA.

(ii) Mechanism : Arenediazonium cations lacking strong electron withdrawing substituents are activated by soft U.V. light with

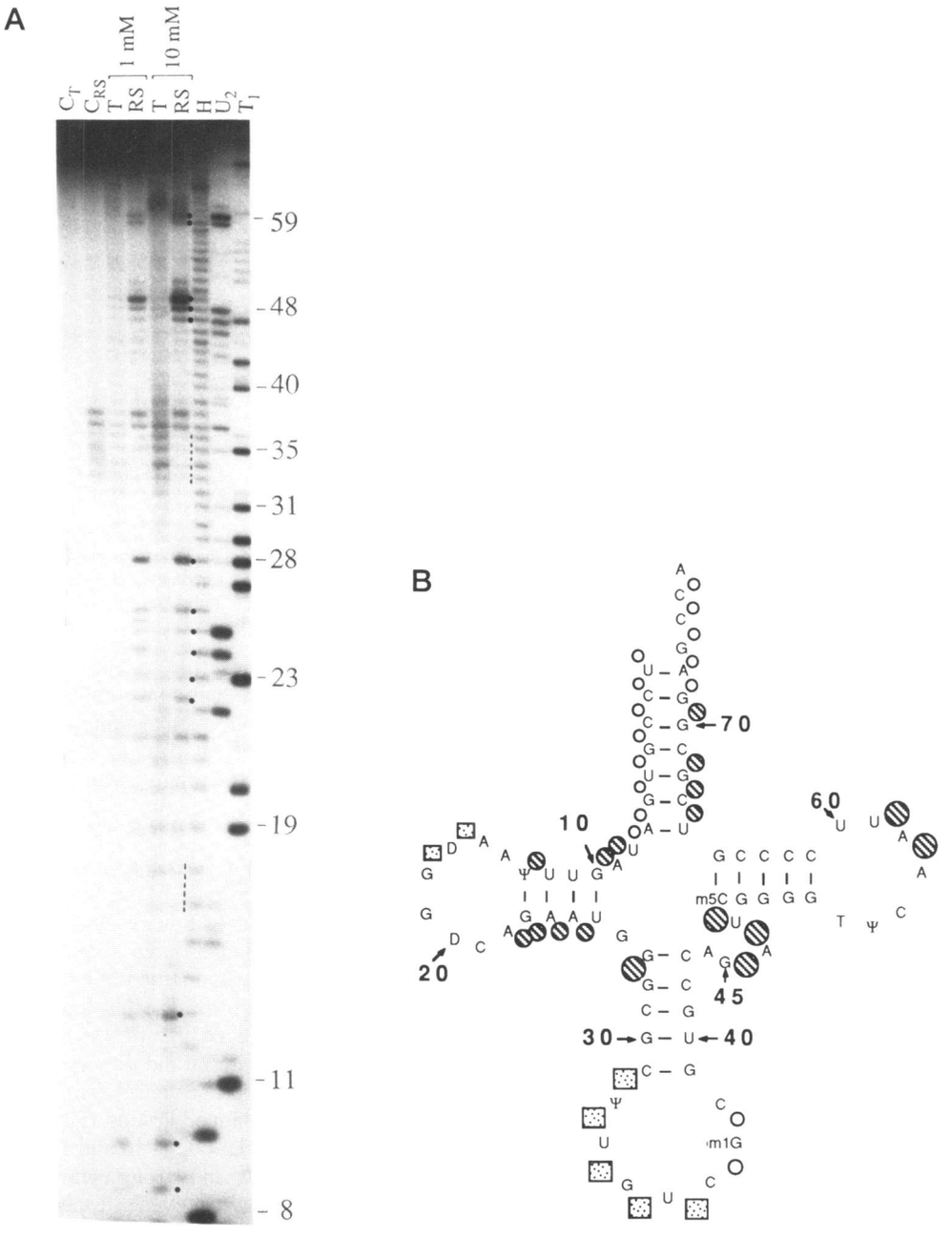

Fig. 2. Mapping of free or complexed $tRNA^{Asp}$ with $BenzN_2^+$. **(A)** Typical autoradiograph of $BenzN_2^+$ experiments performed with 5′ end-labelled $tRNA^{Asp}$. (C_T) Control treatment of tRNA alone ; (C_{RS}) control treatment of tRNA incubated with aspartyl-tRNA synthetase ; (T) mapping of free tRNA and (RS) complexed tRNA with either 1 mM or 10 mM $BenzN_2^+$; (H) formamide ladder ; (U_2) and (T_1) partial ribonuclease U_2 and T_1 digests. Circles indicate enhanced cuts and dotted lines protected phosphates in the presence of the synthetase. The numbering of bands corresponds to that of the phosphates and follows the nomenclature of the tRNA data bank. **(B)** Cloverleaf structure of $tRNA^{Asp}$ (41) showing $BenzN_2^+$ reactivities in the synthetase/RNA complex. The small and large hatched circles represent weak and strong enhanced reactivity and the squares protection in the presence of aspartyl-tRNA synthetase. Empty circles represent regions which could not be tested for methodological reasons.

high quantum yields, leading essentially to nitrogen and arene cations in polar solvents (25). This highly unstable species reacts immediately with a nucleophile in its neighbourhood (lifetime < 0.5 nsec (26)), e.g. water or a proximate group of the nucleic acid. The reaction bears much similarity with the ultimate phosphate alkylating hydrolysis product of ethylnitrosourea, namely ethyldiazonium which thermally decomposes to the ethylcation (27) and shows preferential phosphate *vs* base alkylation. After an irradiation period of < 0.1 to 10 sec, depending on the probe concentration, all the reagent is consumed as seen by bleaching of the chromophore absorption band. This very short reaction time and the low quantities of polyamines needed prevent RNA from hydrolytic degradations appearing essentially in pyrimidine-adenine sequences (e.g. 28), as well as preventing enzymes from inactivation when RNA/protein complexes are studied. Indeed, yeast aspartyl-tRNA synthetase retains 65% of its initial activity after irradiation in the presence of 10 mM $BenzN_2^+$.

For the three probes, experimental conditions were worked out (see Methods section) leading to probe-specific fragmentation

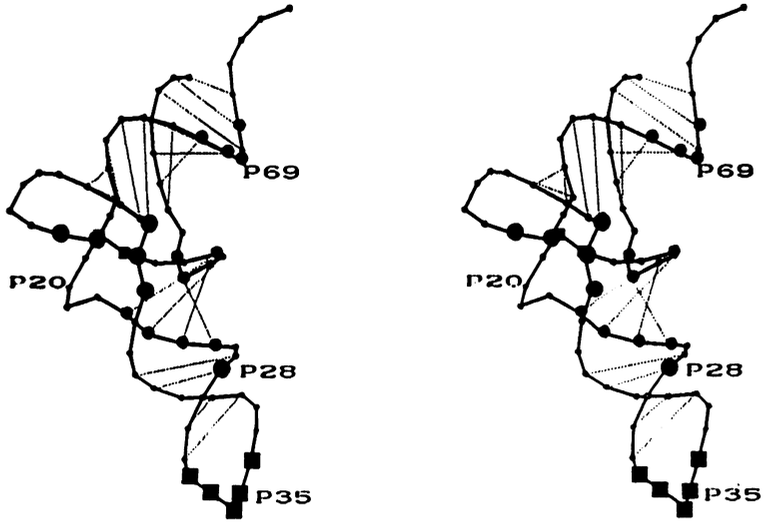

Fig. 3. Footprinting data by $BenzN_2^+$ of $tRNA^{Asp}$ complexed with aspartyl-tRNA synthetase displayed in a stereoview of the three-dimensional backbone of the tRNA. Residues protected by the synthetase are shown by small and large squares ; enhanced reactivities promoted by the synthetase are depicted by small and large circles. The stereoview was drawn with the program PLUTO (S. Motherwell and P. Evans, MRC Cambridge).

patterns of the tRNA. Fragmentation products possess the same electrophoretic mobilities as those generated by ribonuclease T_1 or U_2 limited digestion, except for some small 5′ end-labelled oligoribonucleotides (< 10-mer) (see Fig. 4); also, some 3′ end-labelled tRNA bands are twinned, possibly due to inhomogeneous cleavage on the 5′ site. In general, identical cleavage positions are observed in experiments conducted either with 3′ or 5′ end-labelled tRNA. As a whole, these observations support the following conclusions : (i) cleavage leads to 3′ phosphate oligoribonucleotides; (ii) the polyamines are not attached on the tRNA fragments since electrophoretic mobilities at pH 8.3 are not perturbed by the additional charges which would have been brougth about by the polyamine derivatives ; (iii) most cuts are of primary origin (for a discussion about primary and secondary cuts see ref. 29).

Mapping of $tRNA^{Asp}$ with $BenzN_2^+$

(i) Free tRNA : The arenediazonium derivative used here should act as a photochemically triggered ethylnitrosourea substitute since both compounds are carbocation precursors (see previous section). When used in the range of concentration of ethylnitrosourea ($\approx$ 50 mM), $BenzN_2^+$ gives rise to almost a ladder pattern which highlights its potential use as a photofootprinting reagent for RNA/protein interaction studies (see below). This ladder becomes already apparent at 10 mM of the probe (Fig. 2A). At lower concentrations (1 – < 10 mM, see Fig. 2A), cuts are restricted essentially to the anticodon loop (P32 to P39) and to position P60 in the T-loop, and to a lesser extent to the D-loop and part of the D-stem (P17 to P25 region).

These specific features may be summarized and rationalized as follows : (i) $BenzN_2^+$ shows a definite preference for single stranded loop regions over double stranded stems ; although its electronic properties (high dipole moment, cationic charge) favour intercalation, its small overall surface should direct it towards stacked *single bases* in preference of *base pairs* (see also ref. 10) : hence its selectivity, especially for the anticodon loop. (ii) For most tRNAs tested with ethylnitrosourea, P60 is not alkylated, supporting the hypothesis of an intrinsic T-loop conformation in all tRNAs, stabilized by hydrogen bonding with conserved residues (30). The pocket formed by these neighbouring residues is a favourable structure for increasing the local concentration of the rather lipophilic $BenzN_2^+$, thus enhancing reactivity at this position. Therefore the ability of $BenzN_2^+$ to react strongly with P60 brings an additionnal argument in favour of an intrinsic conformation for the T-loop.

(ii) Transfer RNA^{Asp} bound to aspartyl-tRNA synthetase : To date, structural knowledge of the tRNA/aspartyl-tRNA synthetase complex is limited to low resolution X-ray (31, unpublished results) and ethylnitrosourea footprinting (6) pictures. Both techniques agree with a structure where the nucleic acid lies on the synthetase with the variable loop face in contact with the protein (front side of the tRNA in Fig. 3). We undertook $BenzN_2^+$ footprinting in the presence of excess aspartyl-tRNA synthetase (see experimental section). At 10 mM reagent, strong protection of the anticodon loop (P32 to P36) and a somewhat weaker one in the D-loop (P16 and P18) are noticed (Fig. 2A). Unexpectedly, new and strong cleavage patches appear in the presence of the enzyme, even at 1 mM probe concentration, and spread all over the primary sequence of the RNA (Fig. 2B). When displayed on the three-dimensional structure of $tRNA^{Asp}$, these are concentrated in the front central part of the L-shaped molecule (P9, P10, P13, P28, P46 to P49, P58 and P59) surrounding the variable loop region (Fig. 3). Since the probe is rather lipophilic, it is tempting to suggest that the corresponding contact region of the enzyme is lipophilic too, thus increasing locally the concentration of $BenzN_2^+$ able to react with the tRNA substrate. This hypothesis agrees with the existence of increased stabilities of tRNA/synthetase complexes at very high concentrations of ammonium sulphate as observed elsewhere (32).

Altogether, cleavage protection and enhancement spots give the following minimal contact regions with the enzyme (Fig. 3): most of the anticodon loop (P37 and P38 could not be tested due to degradation), part of the central core formed by the D-, T- and variable loops, and one strand of the D- and acceptor stems which are part of the internal angle of the L-shaped molecule. It is noteworthy that although some regions of the tRNA remain shadowed by the structural probe technique, due to lack of

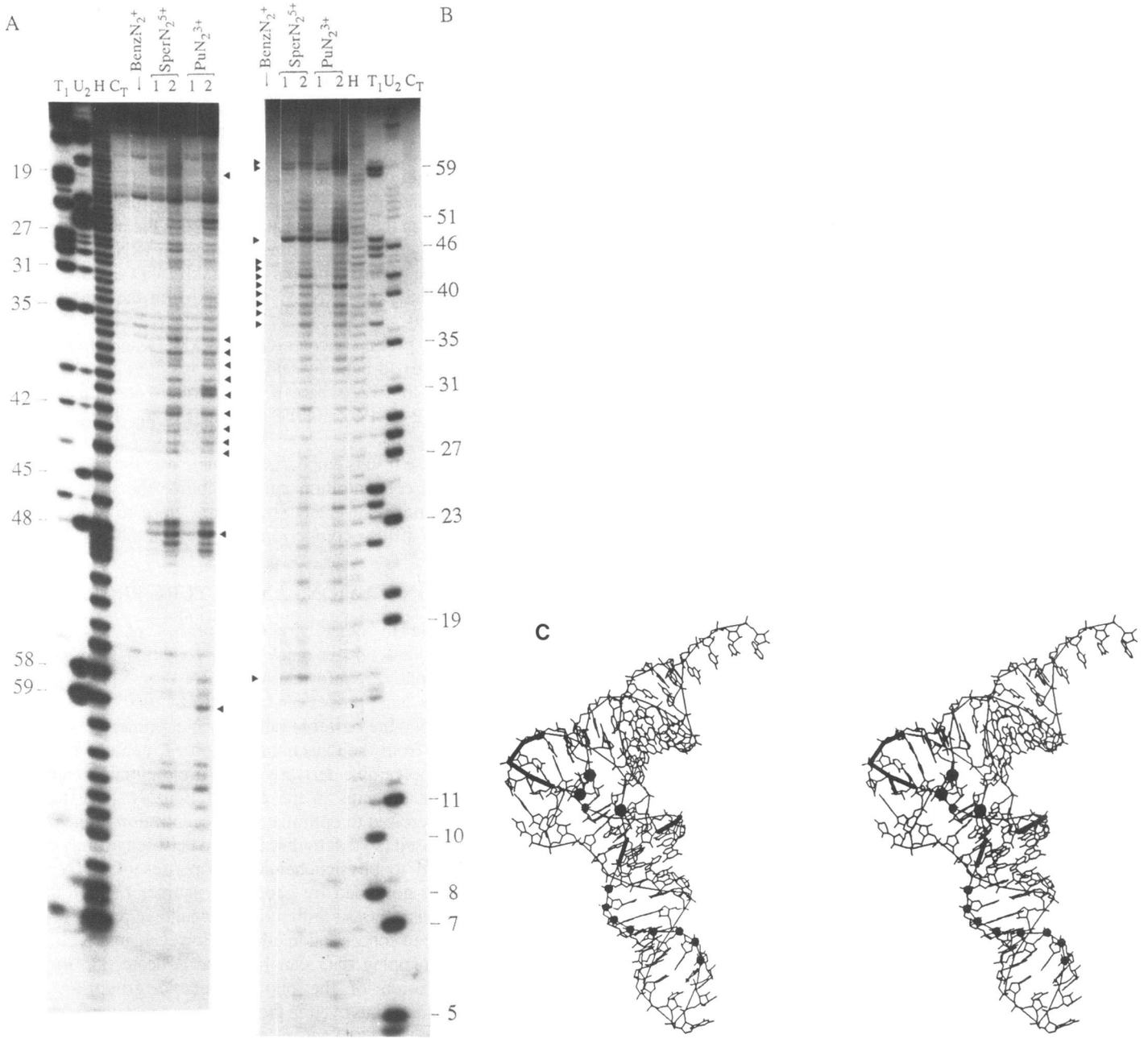

Fig. 4. Location of polyamines in $tRNA^{Asp}$. Autoradiographs of 3′- **(A)** or 5′- **(B)** end-labelled $tRNA^{Asp}$ mapped with the photoactivatable probes. Arrows indicate strong cleavages at 4 μM reagent. (C_T) Control treatment of tRNA ; ($BenzN_2^+$) control experiment to ensure that polyamine reactivity is specific of polyamine-chain affinity : irradiation of $tRNA^{Asp}$ in the presence of 40 μM $BenzN_2^+$ (to be compared with lanes 1 and 2) ; (1) and (2) irradiation of $tRNA^{Asp}$ in the presence of 4 and 40 μM of photoreactive polyamines ($SperN_2^{5+}$ or PuN_2^{3+}) ; (H) formamide ladder ; (U_2) and (T_1) partial ribonuclease U_2 and T_1 digests. **(C)** Major cleavage sites in $tRNA^{Asp}$ by $SperN_2^{5+}$ at 4 μM (spheres) displayed on the stereoview (drawn with the program PLUTO) of the three-dimensional structure of $tRNA^{Asp}$. Bold backbone lines indicate regions which are not cut at 40 μM ; putative spermine sites in the acceptor stem have not been displayed because this region is difficult to map accurately (see text).

experimental data (e.g. at the tRNA extremities), reactivity of the *convex and back* sides of the tRNA are largely unaffected upon binding to the synthetase, and all reactivity changes are located on the *front and concave surface* of the molecule which is along the shortest way from the anticodon to the acceptor ends.

Location of polyamines in $tRNA^{Asp}$

Spermine and polyamines (spermidine, putrescine) in general are ubiquitous biomolecules, especially in the nucleic acid world where they seem to play an important structural role. Yet, although double stranded oligonucleotides and tRNAs crystallize best in the presence of polyamines, little is known about their location and the only structures relevant to this discussion are that of $tRNA^{Phe}$ (33) and of an A-form oligonucleotide (34). $SperN_2^{5+}$ and PuN_2^{3+} possessing unmodified ammonium residues should bind to tRNA with affinity comparable to spermine and putrescine themselves, and their photoreactive moiety should reveal their nucleic acid binding sites rather precisely. Photoaffinity mapping is shown in Fig. 4. Cleavage is already strong in the micromolar range of probe concentration,

three orders of magnitude lower than for $BenzN_2^+$. Natural polyamines are competitors for the photoaffinity polyamines (results not shown) justifying *a posteriori* the specificity of the photochemical cleavages. An overview of the band pattern generated by the two probes shows that spermine and putrescine have identical binding sites of roughly comparable affinities. Thus there is no precise requirement for the polyamine structure in order to bind tRNA. However the reverse is not true : on the nucleic acid side there is a strong selectivity for regions embedded in the three-dimensional structure where the negative charge density is the highest (35). For experiments performed at 4 μM probe concentration, and assuming that cleavage intensity reflects binding strength, the following order of high affinity binding sites is found : P48 >> P59, P60 >> P41 + 3 and P16. Since the reactive diazonium group of the probe is at 4 Å from the polyamine squeleton, these regions must represent independent sites, being more than 10 Å apart from each other.

The strongest spermine induced cleavage site (P48, see Fig. 4) lies where the variable loop faces closely the join between acceptor and D-stems. In the corresponding dense anionic region of the yeast $tRNA^{Phe}$ structure, a spermine molecule has been located (33), curling around P9 to P11 and facing P45 to P47. In the variable loop, nucleotide 47 ($tRNA^{Phe}$) and 48 in $tRNA^{Asp}$ are located in the same region which corresponds to a strong binding site for both tRNAs (in agreement with preliminary data on photocleavage of $tRNA^{Phe}$). Wrapping of the polyamine around P10 considerably reduces its conformational flexibility; this may explain the high cleavage selectivity for P48 with respect to its neighbours, as well as the absence of cleavage on the other strand (P9 to P11) which is on the buried side of the complex where the aryldiazonium residue cannot protrude.

Cleavable residues P59 and P60 are on the T-loop in the heart of the tRNA structure. Here polycationic ammonium substrates may act as a screen between phosphate strings from the D-loop, the 5′ side of the T-stem and the T-loop. On the basis of a space filling representation of this region, it was not possible to distinguish between a two polyamine binding situation, one coming from underneath the D-loop towards the 5′ side of the T-loop (P59) and the other one being in the large cavity capped by the T-arm (P60), or a single polyamine wiggling in the latter.

The P41 region is in the anticodon stem where a second spermine molecule was found in the crystal structure of $tRNA^{Phe}$ (33) between P23 to P26 and P41 to P44 and thus by analogy it can be concluded for $tRNA^{Asp}$ that the polyamine fits into the deep narrow groove joining the anticodon and the D-stems. Here, cleavage is not restricted to a single residue and evenmore the D-stem strand facing the anticodon stem is cleaved too. Such a behaviour reflects conformational and site mobility of the polyamine in agreement with NMR work (36) and is in contrast with the more static X-ray picture. Indeed, an elongated polycation lying along the helix in the major groove of an A-form nucleic acid, as seen in the structure of an oligodeoxyribonucleotide (34), should have enough rotational flexibility to allow the reporter group to reach both strands. On the other hand helicoidal symmetry of the groove with respect to the ribose-phosphate chains should allow fast jumping of the polyamine between isoenergetic binding sites : hence the spread of cleavage sites.

The ends of the primary structure (acceptor stem) are difficult to reach experimentally with accuracy. Nevertheless it can be seen on the gels that here too the cleavage sites are spread along the acceptor stem revealing multiple possible binding sites. This argument is strengthened by X-ray work. Indeed a putative spermine has been located in the electron density map of $tRNA^{Asp}$ (37), the extended molecule lying in the major groove at the P65−67 level. Thus isoenergetic overlapping binding sites for a polyamine on a double stranded nucleic acid may explain why, although polyamines help crystallization, they are so seldom found in the structure.

In its extended conformation, spermine is *ca.* 15 Å long and may span four base pairs. Therefore, assuming that a spermine molecule bound in the anticodon stem excludes the neighbouring binding sites, there are 3−4 binding sites on $tRNA^{Asp}$ in the 1−10 μM range. This compares favourably with a value of 3 in the 10 μM range for $tRNA^{Phe}$ (38) and 6 in the mM range for $tRNA^{Ileu}$ (39).

At the higher probe concentration (40 μM, where $BenzN_2^+$ is still ineffective) all but a few phosphate residues are cleaved. These are P10 to P12 (where a Mg^{2+} ion is coordinated in $tRNA^{Phe}$ (33)), P45, P46 and the outer half of the T-loop from P54 to P58 (Fig. 4).

Altogether these results emphasize a double role for polyamines at physiological concentration : they stabilize the structure of nucleic acids where phosphate strands are close to each other and they act as diffuse counterions for the anionic polymers.

GENERAL CONCLUSIONS AND FUTURE PROSPECTS

When compared to other structural probes of RNA, the aryldiazonium salts act under much milder conditions, thus better preserving the native conformation of RNA or RNA/protein complexes. Also, these probes can be efficiently used over a large pH range provided the buffer is not too nucleophilic. However, to benefit fully from their peculiar properties, namely affinity binding for the polyamine derivatives and preferential selectivity for hydrophobic domains in the case of $BenzN_2^+$, particular care must be exercised to optimize the concentration range over which they are used (so that to discriminate between affinity type reactions related to physicochemical properties of RNA and reactivities only governed by geometric characteristics of the nucleic acid). This contrasts with more conventional probes which are less sensitive to concentration effects. However, interpretation of polyamine mapping data can be more delicate due to the asymmetric location of the photoactivatable group on the polycationic chains : thus even in the case of an unique polyamine site on the nucleic acid two cuts may be generated corresponding to the two alternate locations of the probe.

As to $BenzN_2^+$ it is important to emphasize that both structural mapping data of free $tRNA^{Asp}$ and footprinting of the tRNA complexed to aspartyl-tRNA synthetase, agree with structural conclusions obtained with ethylnitrosourea probing (6), although the diazonium derivative yields additional informations linked to its lipophilic character. This is a good prerequisite for using $BenzN_2^+$ to probe conformational features on other RNAs. Preliminary studies along this line, for example as to the conformation of T-loops in tRNAs, yielded similar reactivities of P60 within both the $tRNA^{Asp}$ *in vitro* trancript lacking the modified bases and the modified species, suggesting similar conformations of this region in modified and unmodified $tRNA^{Asp}$. From another point of view, photoactivatable aryldiazonium salts may be straigthforward reagents to probe RNAs over their thermal stability range since cleavage reactions are already fast at room temperature. Further, the polyamine derivatives are potentialy efficient tools to localize precisely

binding sites of natural polyamines in RNAs, in particular in the case of plant viral RNAs which are known to bind a great number of such molecules (40 and ref. included). Experiments are underway to explore these different possibilities.

ACKNOWLEDGEMENTS

We thank Philippe Dumas, Anne Catherine Dock-Brégeon and Eric Westhof for helpful and stimulating discussions. This work was supported by the Centre National de la Recherche Scientifique and the Université Louis Pasteur (Strasbourg). A. G. was supported by a grant from the MRES.

REFERENCES

1. Kirkegaard, K., Buc, H., Spassky, A. and Wang, J.C. (1983) Proc. Natl. Acad. Sci. USA, **80**, 2544–2548.
2. Ehresmann, C., Baudin, F., Mougel, M., Romby, P., Ebel, J.P. and Ehresmann, B. (1987) Nucleic Acids Res., **15**, 9109–9128.
3. Romby, P., Moras, D., Dumas, P., Ebel, J.P. and Giegé, R. (1987) J. Mol. Biol., **195**, 193–204.
4. Siebenlist, U. and Gilbert, W. (1980) Proc. Natl. Acad. Sci. USA, **77**, 122–126.
5. Bushman, F.D., Anderson, J.E., Harrison, S.C. and Ptashne, M. (1985) Nature, **316**, 651–653.
6. Romby, P., Moras, D., Bergdoll, M., Dumas, P., Vlassov, V.V., Westhof, E., Ebel, J.P. and Giegé, R. (1985) J. Mol. Biol., **184**, 455–471.
7. Théobald, A., Springer, M., Grunberg-Manago, M., Ebel, J.P. and Giegé, R. (1988) Eur. J. Biochem., **175**, 511–524.
8. Maxam, A.M. and Gilbert, W. (1977) Proc. Natl. Acad. Sci. USA , **74**, 560–564.
9. Peattie, D.A. (1979) Proc. Natl. Acad. Sci. USA, **76**, 1760–1764.
10. Behr, J.P. (1989) J. Chem. Soc., Chem. Comm., 101–103.
11. Moras, D., Thierry, J.C., Comarmond, M.B., Fischer, J., Weiss, R., Ebel, J.P. and Giegé, R. (1980) Nature, **288**, 669–674.
12. Westhof, E., Dumas, P. and Moras, D. (1985) J. Mol. Biol., **184**, 119–145.
13. Goeldner, D.G. and Hirth, C.G. (1980) Proc. Natl. Acad. Sci. USA, **77**, 6439–6442.
14. Dirheimer, G. and Ebel, J.P. (1967) Bull. Soc. Chim. Biol., **49**, 1679–1686.
15. Keith, G., Gangloff, J. and Dirheimer, G. (1971) Biochimie, **53**, 123–125.
16. Giegé, R., Dock, A.C., Kern, D., Lorber, B., Thierry, J.C. and Moras D. (1986) J. Crystal Growth, **76**, 554–561.
17. Lorber, B., Kern, D., Dietrich, A., Gangloff, J., Ebel, J.P. and Giegé, R. (1983) Biochem. Biophys. Res. Commun., **117**, 259–267.
18. Ruff, M., Cavarelli, J., Mikol, V., Lorber, B., Mitschler, A., Giegé, R., Thierry, J.C. and Moras, D. (1988) J. Mol. Biol., **201**, 235–236.
19. Rether, B., Bonnet, J. and Ebel, J.P. (1974) Eur. J. Biochem., **50**, 281–288.
20. Silberklang, M., Gillam, A.M. and Rajbhandary, U.L. (1977) Nucleic Acids Res., **4**, 4091–4108.
21. Bonnet, J. and Ebel, J.P. (1975) Eur. J. Biochem., **58**, 193–201.
22. Kuokkanen, T. (1987) Finnish Chem. Letters, **14**, 184–192.
23. Morgan, J.E., Blankenship, J.W. and Matthews, H.R. (1986) Arch. Biochem. Biophys., **246**, 225–232.
24. Tometsko, A.M., Turuka, J. and Comstock, J. (1978) Int. J. Pept. Res., **12**, 143–148.
25. Ando, W., *in* 'The Chemistry of Functional Groups : Diazonium and Diazo', Patai, W., New-York, 1978.
26. Scaiano, J.C. and Kim-Thuan, N. (1983) J. Photochem., **23**, 269–276.
27. Singer, B. (1976) Nature, **264**, 333–339.
28. Moras, D., Dock, A.C., Dumas, P., Westhof, E., Romby, P. and Giegé, R. (1983) *in* 'Nucleic Acids : The Vectors of Life' (Pullman, B. and Jortner, J., eds), **16**, pp. 403–414, Reidel Publishing Co., Dordrecht.
29. Favorova, O.O, Fasiolo, F., Keith, G., Vassilenko, S.K. and Ebel, J.P. (1974) Biochemistry, **20**, 1006–1011.
30. Romby, P., Carbon, P., Westhof, E., Ehresmann, C., Ebel, J.P., Ehresmann, B. and Giegé, R. (1987) J. Biomol. Struct. Dyn., **5**, 669–687.
31. Podjarny, A., Rees, B., Thierry, J.C., Cavarelli, J., Jesior, J.C., Roth, M., Lewitt-Bentley, A., Kahn, R., Lorber, B., Ebel, J.P., Giegé, R. and Moras, D. (1987) J. Biomol. Sruct. Dyn., **5**, 187–198.
32. Giegé, R., Lorber, B., Ebel, J.P., Moras, D., Thierry, J.C., Jacrot, B. and Zaccaï, G. (1982) Biochimie, **64**, 357–362.
33. Quigley, G.M., Teeter, M. and Rich, A. (1978) Proc. Natl. Acad. Sci. USA, **75**, 64–68.
34. Jain, S., Zon, G. and Sundaralingam, M. (1989) Biochemistry, **28**, 2360–2364.
35. Zakrzewska, K. and Pullman, B. (1986) Biopolymers, **25**, 375–392.
36. Wemmer, D.E., Srivenugopal, K.S., Reid, B.R. and Morris, D. (1985) J. Mol. Biol., **185**, 457–459.
37. Dumas, P. (1986) Thèse de Doctorat d'Etat, Université Louis Pasteur, Strasbourg (France).
38. Sakai, T.T. and Cohen S.S. (1976) Progr. Nucl. Acids Res. Mol. Biol., **17**, 15–43.
39. Takeda,Y. and Ohnishi, T. (1975) Biochem. Biophys. Res. Comm., **63**, 611–617.
40. Eecen, H.G., Van Dietendonck, J.H., Pleij, C.W.A., Mandel, M. and Bosch, L. (1985) Biochemistry, **24**, 3610–3617.
41. Keith, G., Gangloff, J. and Dirheimer, G. (1971) Biochimie, **53**, 123–125.